

**Faradaic deionization of brackish and sea water
via pseudocapacitive cation and anion intercalation
into few layered molybdenum disulfide**

Pattarachai Srimuk,^{1,2} Juhan Lee,^{1,2} Simon Fleischmann,^{1,2} Soumyadip Choudhury,¹
Nicolas Jäckel,^{1,2} Marco Zeiger,^{1,2} Choonsoo Kim,¹ Mesut Aslan,¹ Volker Presser^{1,2,*}

Supporting Information

Calculation of salt adsorption capacity and charge efficiency

$$SAC = \frac{v \cdot M_{NaCl}}{m_{total}} \int c dt. \quad \text{Equation (S1)}$$

In this equation, v is the flow rate (mL/min), M_{NaCl} is molecular weight of NaCl (58.44 g/mol), m_{total} is total mass of electrodes (g), t is the time over the adsorption step (min), and c is the concentration of NaCl (mmol/L).

The concentration of NaCl is calculated by relation of concentration and conductivity:

$$c = \left(\frac{\sigma - 4.5}{121.29} \right)^{1/0.9826} - 0.13 \quad \text{Equation (S2)}$$

where σ is actual conductivity ($\mu\text{S}/\text{cm}$) which subtracts the conductivity by the conductivity of water by measured pH from the measured conductivity:

$$\sigma = \sigma_m - \sigma_w \quad \text{Equation (S3)}$$

where σ_m is measured conductivity (mS/cm) and σ_w is the conductivity of water calculated by:

$$\sigma_w = \frac{e^2}{k_B T} \left(10^{pH} \cdot N_A \cdot D_{H_3O^+} + \frac{10^{-14}}{10^{-pH}} \cdot N_A \cdot D_{OH^-} \right) \quad \text{Equation (S4)}$$

where k_B is Boltzmann constant ($1.38 \cdot 10^{-23} \text{ m}^2 \text{ kg} / \text{ s}^2 \text{ K}$), N_A is Avogadro constant ($6.02 \cdot 10^{23} \text{ mol}^{-1}$), $D_{H_3O^+}$ is diffusion coefficient of hydronium ion ($9.3 \cdot 10^{-9} \text{ m}^2 / \text{ s}$), and D_{OH^-} is the diffusion coefficient of an hydroxyl ion ($5.3 \cdot 10^{-9} \text{ m}^2 / \text{ s}$).

$$\text{Charge efficiency (\%)} = \left(\frac{\frac{SAC \left(\frac{mg}{g} \right)}{M_{NaCl} \left(\frac{g}{mol} \right)}}{\frac{\text{Specific capacitance} \left(\frac{C}{g \cdot V} \right) \cdot \text{Cell coltage (V)}}{4 \cdot \text{Faraday constant} \left(\frac{C}{mol} \right)}} \right) \cdot 100 \quad \text{Equation (S5)}$$

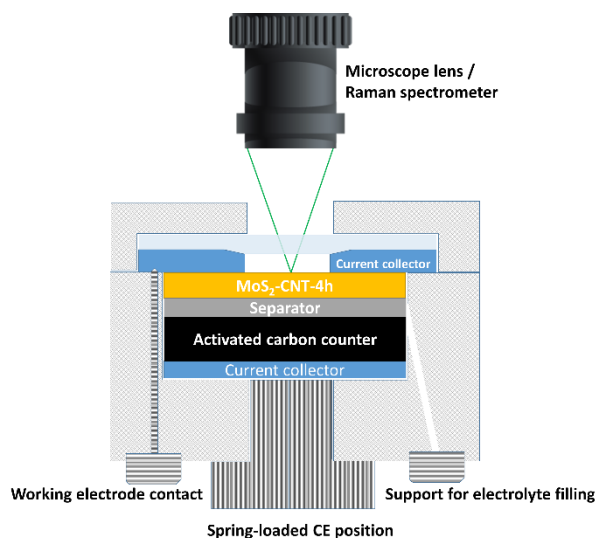


Figure S1. Schematic configuration of the electrochemical in situ stage for Raman spectroscopy.

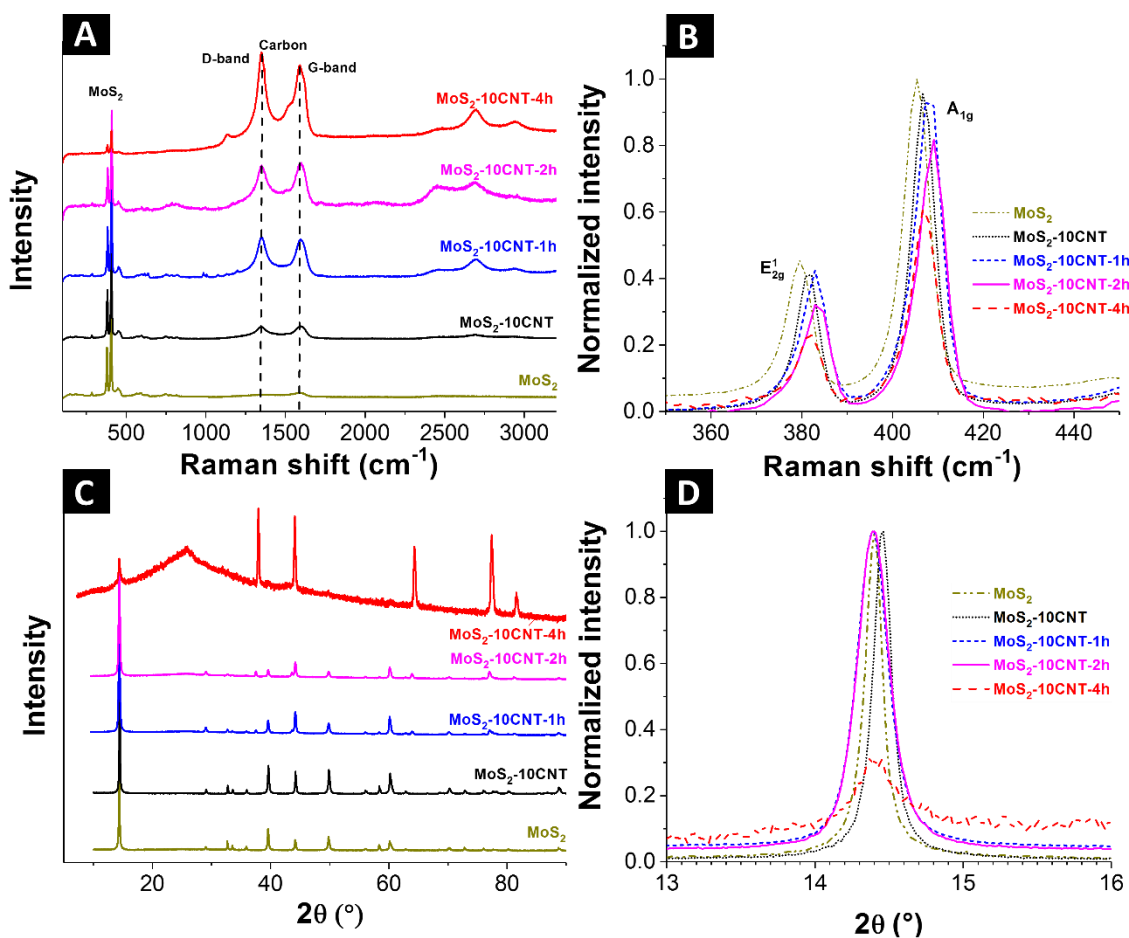


Figure S2 Raman spectra (A) and (B), X-ray diffractogram of MoS₂, MoS₂-10CNT, and electrochemically activated samples (i.e., MoS₂-10CNT-1h, MoS₂-10CNT-2h, MoS₂-10CNT-4h).

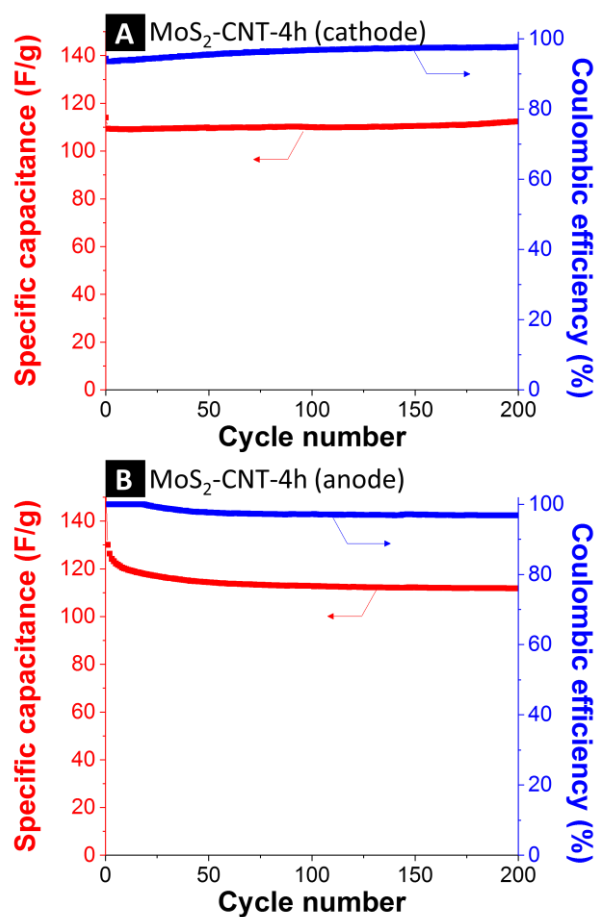


Figure S3 Cyclic stability of MoS₂-10CNT-4h at 0.5 A/g in 1 M NaCl. (A) Cathode, (B) anode.

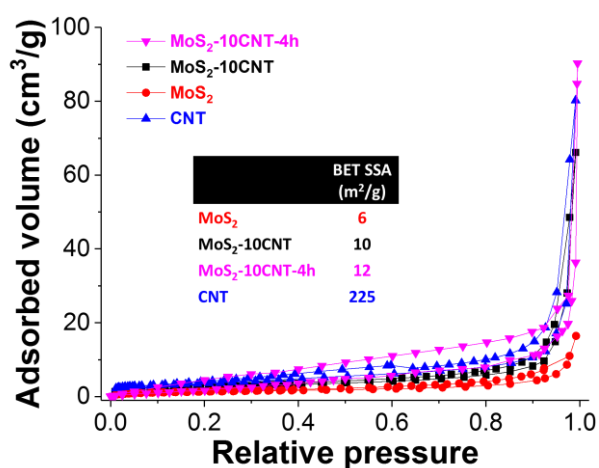


Figure S4. Nitrogen gas sorption isotherm recorded at -196 °C of MoS₂, MoS₂-10CNT, MoS₂-10CNT-4h, and pure carbon nanotubes (CNT).

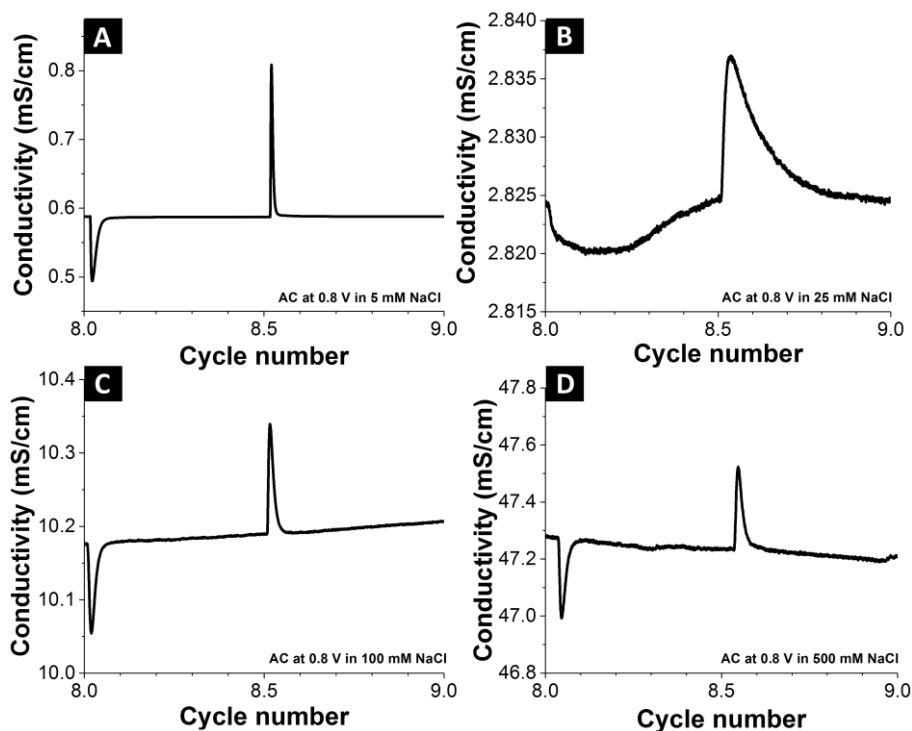


Figure S5. CDI performance of AC at 0.8 V charging and 0 V discharging in (A) 5 mM NaCl, (B) 25 mM NaCl, (C) 100 mM NaCl, and (D) 500 mM NaCl.

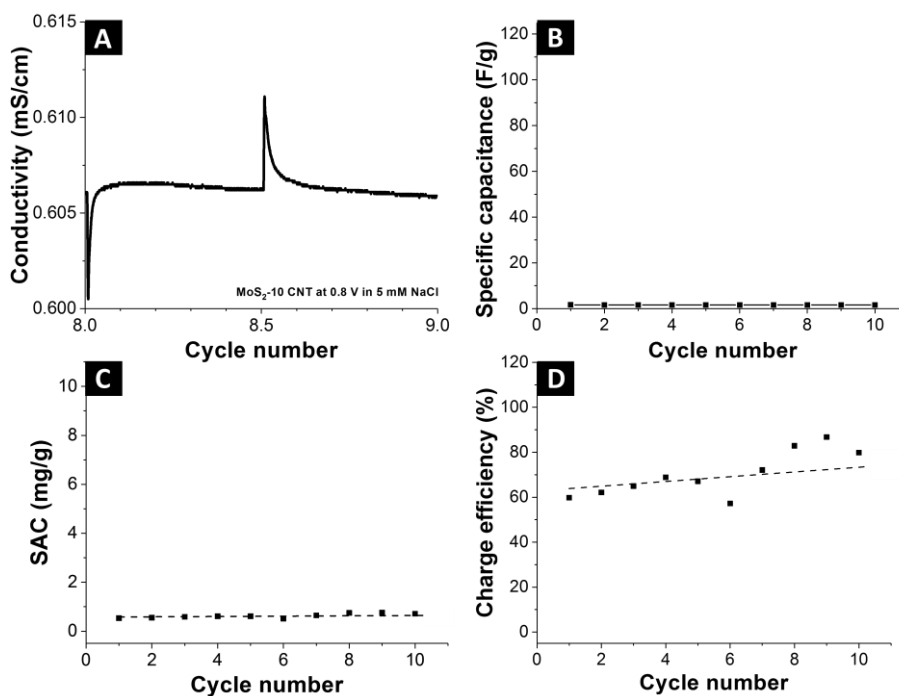


Figure S6. (A) CDI performance of MoS₂-10CNT at 0.8 V charging and 0 V discharging in 5 mM NaCl, (B) specific capacitance from CDI cell, (C) salt adsorption capacity (SAC), and (D) CDI charge efficiency.

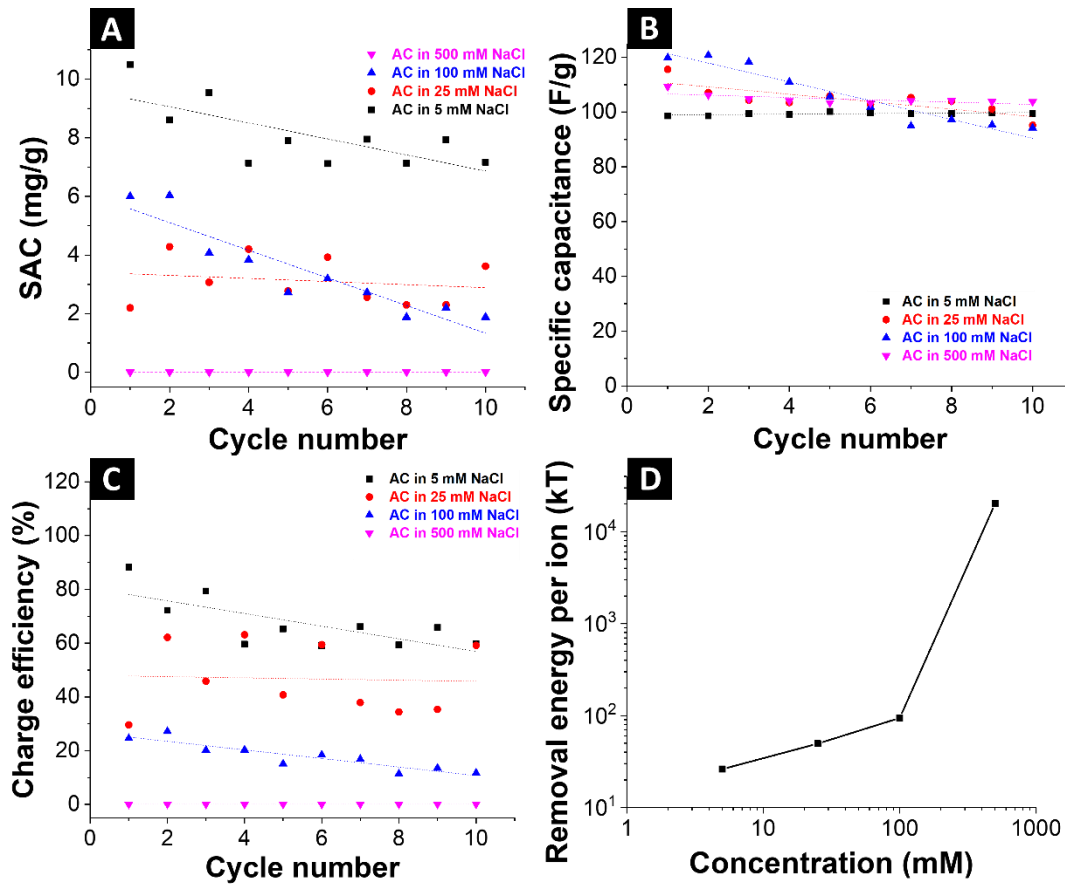


Figure S7. Comparative data for CDI with activated carbon (AC). (A) Salt adsorption capacity (SAC), (B) specific capacitance from CDI cell, (C) charge efficiency, and (D) energy per ion removed of AC electrode in different salt concentration.

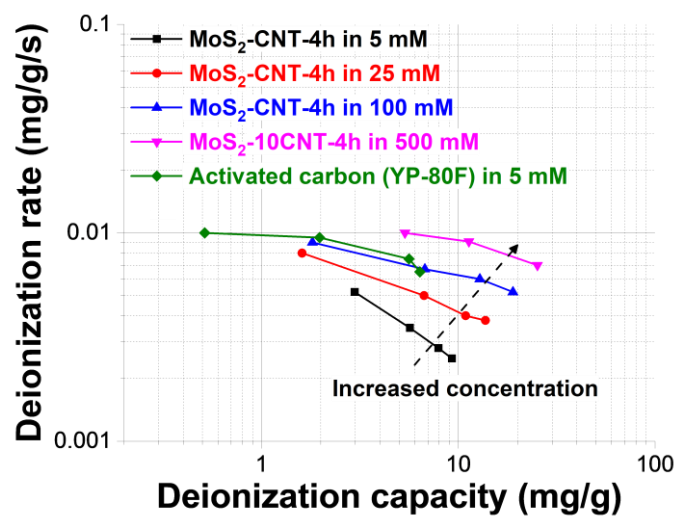


Figure S8. Kim-Yoon-Plot ("CDI Ragone plot" for FDI at different molar concentrations.

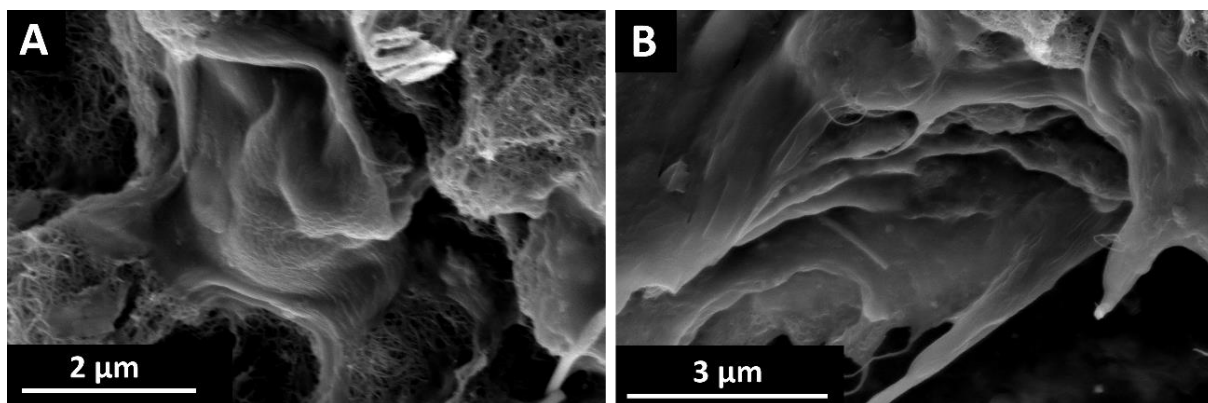


Figure S9. Post mortem scanning micrographs (A) negative electrode MoS₂-10CNT-4h, and (B) positive electrode MoS₂-10CNT-4h.